Swin Transformer

Ze Liu Yutong Lin Yue Cao Han Hu Yixuan Wei Zheng Zhang Stephen Lin Baining Guo

Swin Transformer : Hierarchical Vision Transformer using Shifted Windows. ICCV 2021

https://arxiv.org/abs/2103.14030

Swin Transformer

- State of the Art | Object Detection on COCO test-dev (using additional training data)
- State of the Art | Instance Segmentation on COCO test-dev
- State of the Art | Semantic Segmentation on ADE20K (using additional training data)
- Ranked #3 | Action Classification on Kinetics-400 (using additional training data)

腾讯课堂

> **Image Classification**: Included in this repo. See get_started.md for a quick start.

> **Object Detection and Instance Segmentation**: See Swin Transformer for Object Detection.

> **Semantic Segmentation**: See Swin Transformer for Semantic Segmentation.

> **Video Action Recognition**: See Video Swin Transformer.

> **Semi-Supervised Object Detection**: See Soft Teacher.

> **SSL: Contrasitive Learning**: See Transformer-SSL.

> 🔥 **SSL: Masked Image Modeling**: See SimMIM.

Problems of ViT

- Does not consider the difference between textual and visual signals
- Mainly for image classification

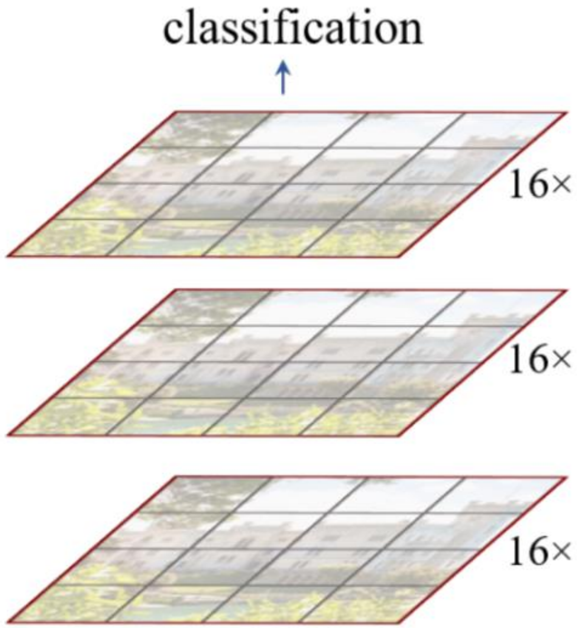

ViT

good priors for visual signals
(hierarchy / locality /
translation invariance)

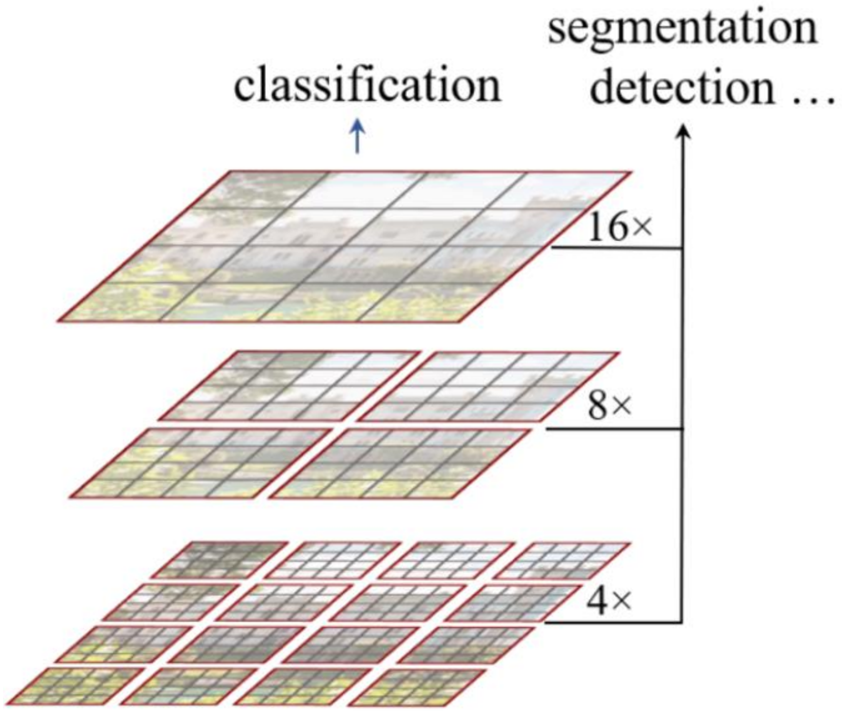

Swin Transformer

Key tech innovation : locality by Shifted windows

- Non-overlapped windows (faster real speed than sliding windows)
- Windows are shifted in the next layer

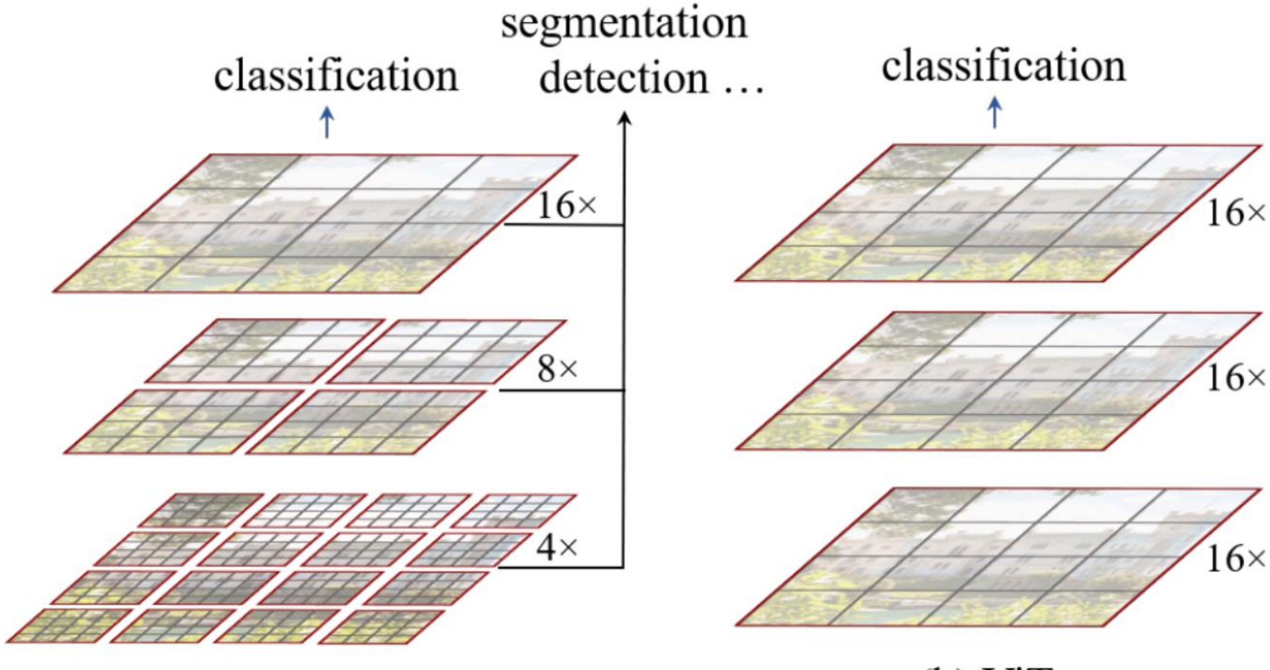

(a) Swin Transformer (ours)   (b) ViT

- Hierarchical feature maps
- Windows Multi-Head Self-Attention (W-MSA)
  Shifted Windows Multi-Head Self-Attention (SW-MSA)

Key tech innovation：locality by Shifted windows

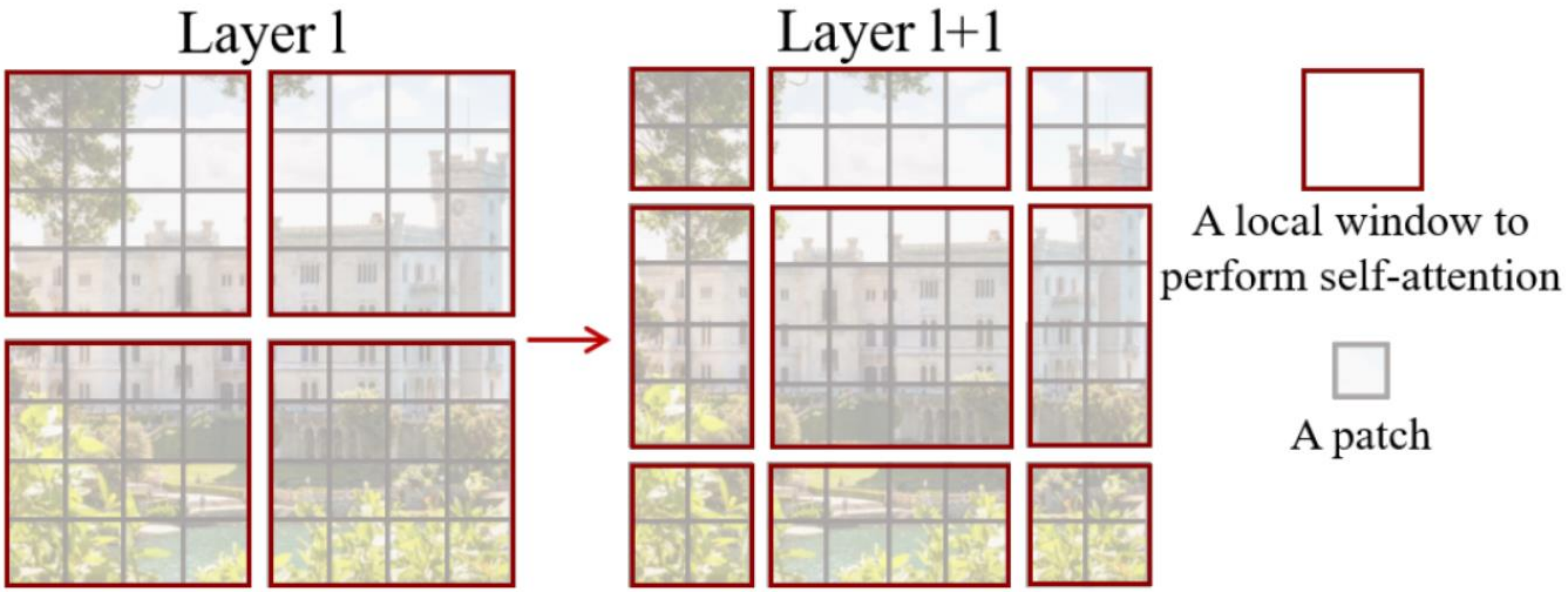

1）自注意的计算在局部的非重叠窗口内进行。不同query会共享同样的key集合，从而对硬件友好

2）在前后两层的Transformer模块中，非重叠窗口的配置相比前一层做了半个窗口的移位，使得上一层中不同窗口的信息进行了交换。

Self-attention in non-overlapped windows

For efficient modeling, we propose to compute self attention within local windows.

The windows are arranged to evenly partition the image in a non-overlapping manner.

Supposing each window contains M × M patches, the computational complexity of a global MSA module and a window based one on an image of h × w patches are :

$$\Omega(\text{MSA}) = 4hwC^2 + 2(hw)^2 C, \qquad (1)$$

$$\Omega(\text{W-MSA}) = 4hwC^2 + 2M^2 hwC, \qquad (2)$$

where the former is quadratic to patch number hw, and the latter is linear when M is fixed (set to 7 by default). Global self-attention computation is generally unaffordable for a large hw, while the window based self-attention is scalable.

The architecture of a Swin Transformer (Swin-T)

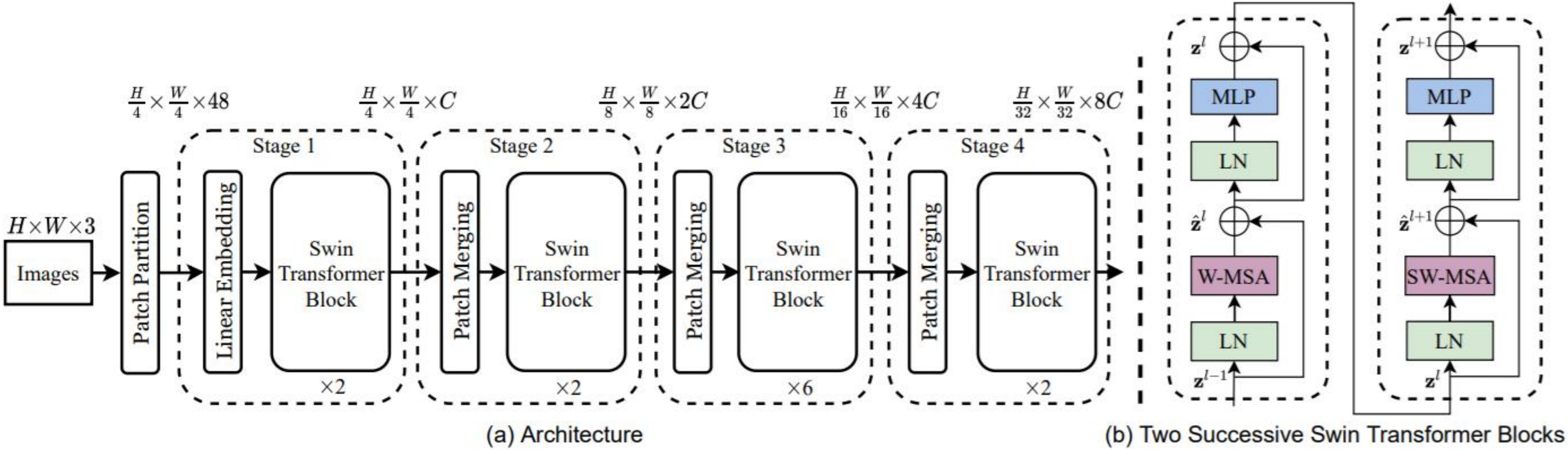

Figure 3. (a) The architecture of a Swin Transformer (Swin-T); (b) two successive Swin Transformer Blocks (notation presented with Eq. (3)). W-MSA and SW-MSA are multi-head self attention modules with regular and shifted windowing configurations, respectively.

Patch Merging

经过Patch Merging后，feature map的高和宽会减半，深度会加倍

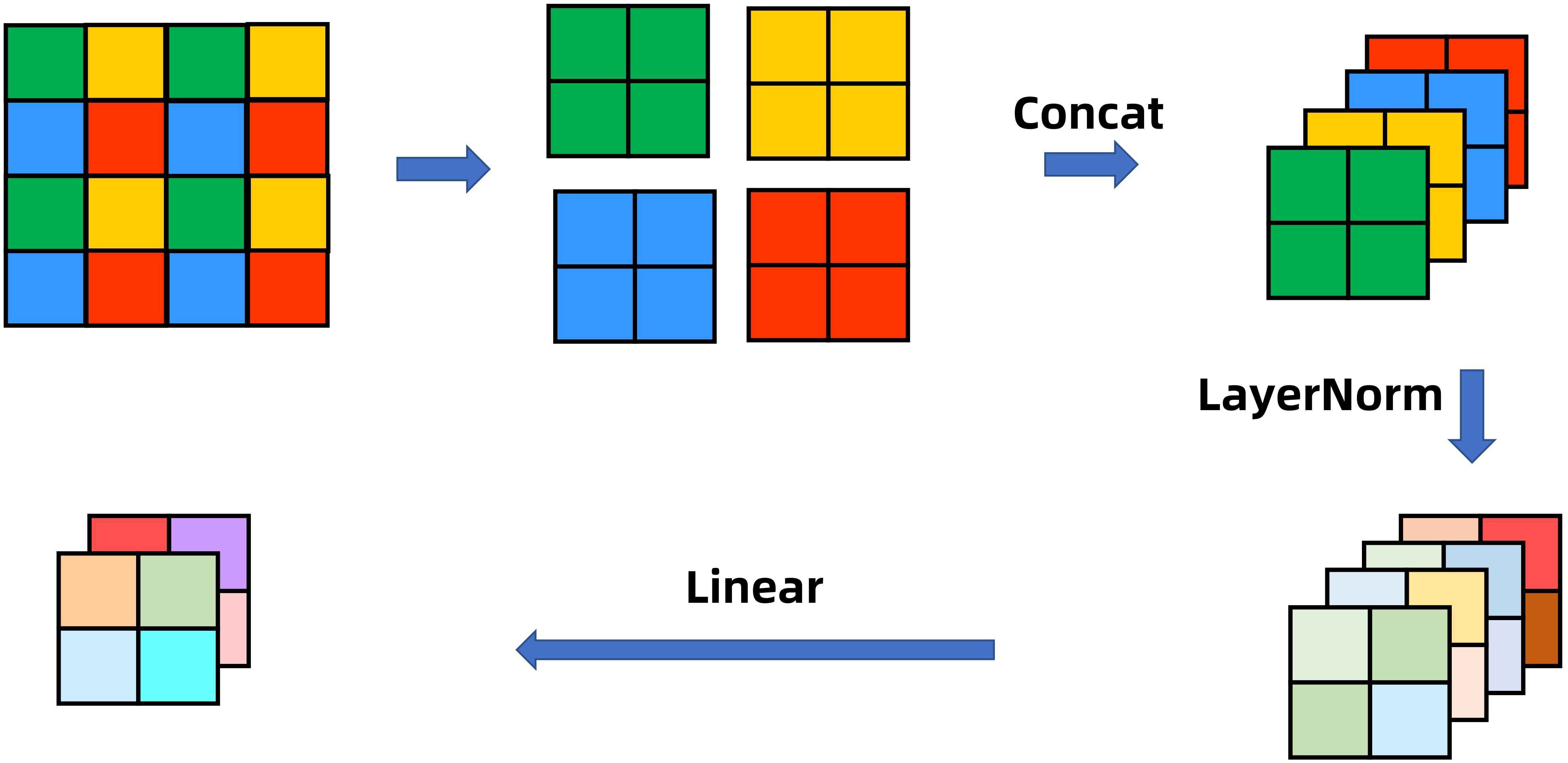

Swin Transformer block

Swin Transformer is built by replacing the standard **multi-head self attention (MSA)** module in a Transformer block by a module based on shifted windows, with other layers kept the same.

A Swin Transformer block consists of a shifted window based MSA module, followed by a 2-layer MLP with GELU nonlinearity in between.

A LayerNorm (LN) layer is applied **before** each MSA module and each MLP, and a residual connection is applied after each module.

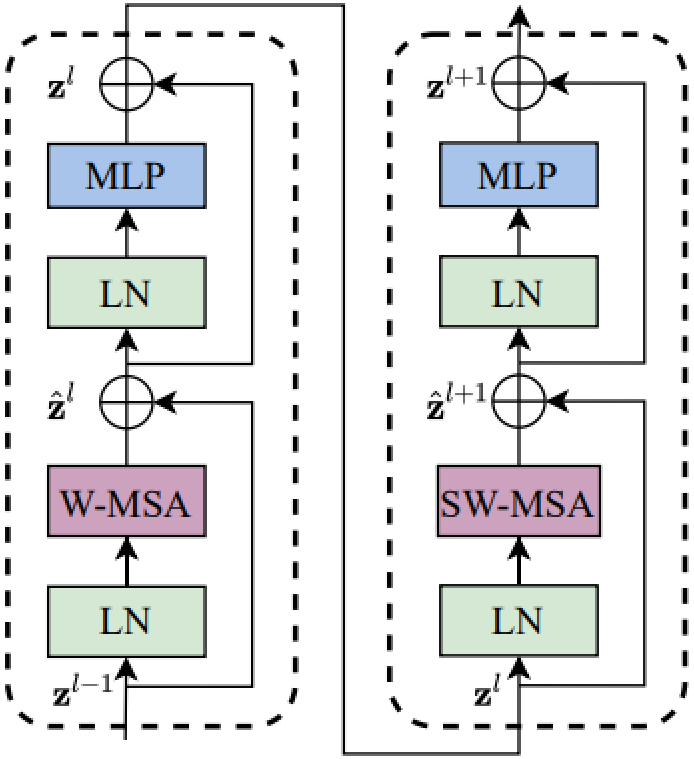

Shifted window partitioning in successive blocks

With the shifted window partitioning approach, consecutive Swin Transformer blocks are computed as

$$\hat{\mathbf{z}}^{l} = \text{W-MSA}\left(\text{LN}\left(\mathbf{z}^{l-1}\right)\right) + \mathbf{z}^{l-1},$$
$$\mathbf{z}^{l} = \text{MLP}\left(\text{LN}\left(\hat{\mathbf{z}}^{l}\right)\right) + \hat{\mathbf{z}}^{l},$$
$$\hat{\mathbf{z}}^{l+1} = \text{SW-MSA}\left(\text{LN}\left(\mathbf{z}^{l}\right)\right) + \mathbf{z}^{l},$$
$$\mathbf{z}^{l+1} = \text{MLP}\left(\text{LN}\left(\hat{\mathbf{z}}^{l+1}\right)\right) + \hat{\mathbf{z}}^{l+1},$$

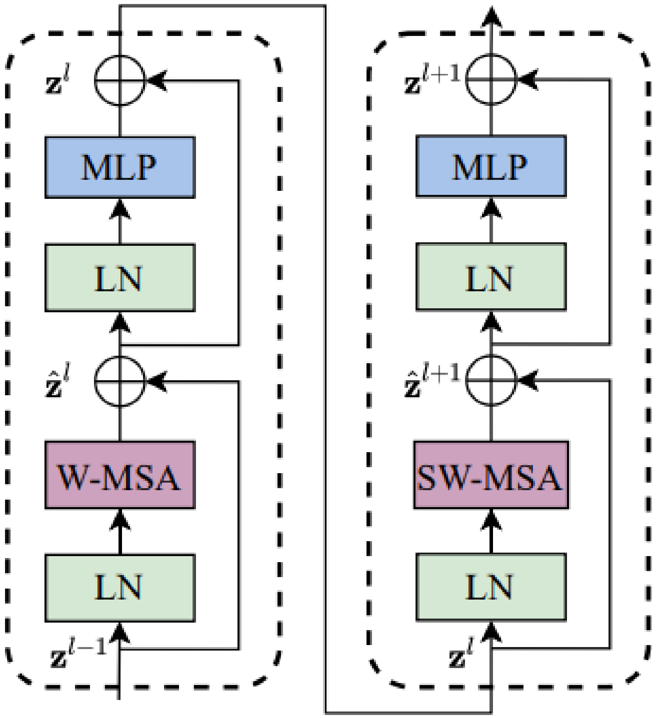

where $\hat{\mathbf{z}}^{l}$ and $\mathbf{z}^{l}$ denote the output features of the (S)W-MSA module and the MLP module for block l, respectively;

Swin T(Tiny)，S(Small)，B(Base)，L(Large)

	downsp. rate (output size)	Swin-T	Swin-S	Swin-B	Swin-L
stage 1	4× (56×56)	concat 4×4, 96-d, LN	concat 4×4, 96-d, LN	concat 4×4, 128-d, LN	concat 4×4, 192-d, LN
		[win. sz. 7×7, dim 96, head 3] × 2	[win. sz. 7×7, dim 96, head 3] × 2	[win. sz. 7×7, dim 128, head 4] × 2	[win. sz. 7×7, dim 192, head 6] × 2
stage 2	8× (28×28)	concat 2×2, 192-d , LN	concat 2×2, 192-d , LN	concat 2×2, 256-d , LN	concat 2×2, 384-d , LN
		[win. sz. 7×7, dim 192, head 6] × 2	[win. sz. 7×7, dim 192, head 6] × 2	[win. sz. 7×7, dim 256, head 8] × 2	[win. sz. 7×7, dim 384, head 12] × 2
stage 3	16× (14×14)	concat 2×2, 384-d , LN	concat 2×2, 384-d , LN	concat 2×2, 512-d , LN	concat 2×2, 768-d , LN
		[win. sz. 7×7, dim 384, head 12] × 6	[win. sz. 7×7, dim 384, head 12] × 18	[win. sz. 7×7, dim 512, head 16] × 18	[win. sz. 7×7, dim 768, head 24] × 18
stage 4	32× (7×7)	concat 2×2, 768-d , LN	concat 2×2, 768-d , LN	concat 2×2, 1024-d , LN	concat 2×2, 1536-d , LN
		[win. sz. 7×7, dim 768, head 24] × 2	[win. sz. 7×7, dim 768, head 24] × 2	[win. sz. 7×7, dim 1024, head 32] × 2	[win. sz. 7×7, dim 1536, head 48] × 2

Table 7. Detailed architecture specifications.

- win. sz. 7x7表示使用的窗口（Windows）的大小
- dim表示feature map的channel深度）
- head表示多头注意力模块中head的个数

Architecture Variants

- Swin-T: $C = 96$, layer numbers = $\{2, 2, 6, 2\}$
- Swin-S: $C = 96$, layer numbers =$\{2, 2, 18, 2\}$
- Swin-B: $C = 128$, layer numbers =$\{2, 2, 18, 2\}$
- Swin-L: $C = 192$, layer numbers =$\{2, 2, 18, 2\}$

where C is the channel number of the hidden layers in the first stage.

The window size is set to $M = 7$ by default. The query dimension of each head is $d = 32$, and the expansion layer of each MLP is $\alpha = 4$.

腾讯课堂

Efficient batch computation for shifted configuration An issue with shifted window partitioning is that it will result in more windows, from $\lceil \frac{h}{M} \rceil \times \lceil \frac{w}{M} \rceil$ to $(\lceil \frac{h}{M} \rceil + 1) \times (\lceil \frac{w}{M} \rceil + 1)$ in the shifted configuration, and some of the windows will be smaller than $M \times M$[4]. A naive solution is to

[4]To make the window size (M, M) divisible by the feature map size of (h, w), bottom-right padding is employed on the feature map if needed.

Illustration of an efficient batch computation approach for self-attention in shifted window partitioning

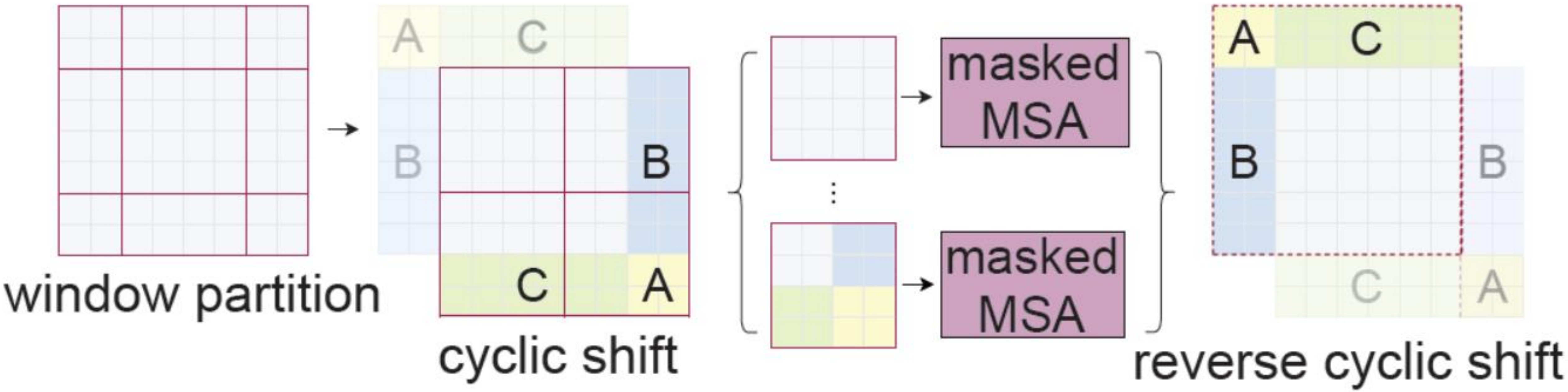

Relative position bias In computing self-attention, we follow [49, 1, 32, 33] by including a relative position bias $B \in \mathbb{R}^{M^2 \times M^2}$ to each head in computing similarity:

$$\text{Attention}(Q, K, V) = \text{SoftMax}(QK^T/\sqrt{d} + B)V, \quad (4)$$

where $Q, K, V \in \mathbb{R}^{M^2 \times d}$ are the *query*, *key* and *value* matrices; d is the *query*/*key* dimension, and M^2 is the number of patches in a window. Since the relative position along each axis lies in the range $[-M+1, M-1]$, we parameterize a smaller-sized bias matrix $\hat{B} \in \mathbb{R}^{(2M-1)\times(2M-1)}$, and values in B are taken from $\hat{B}$.

Gaussian Error Linear Unit (GELU)

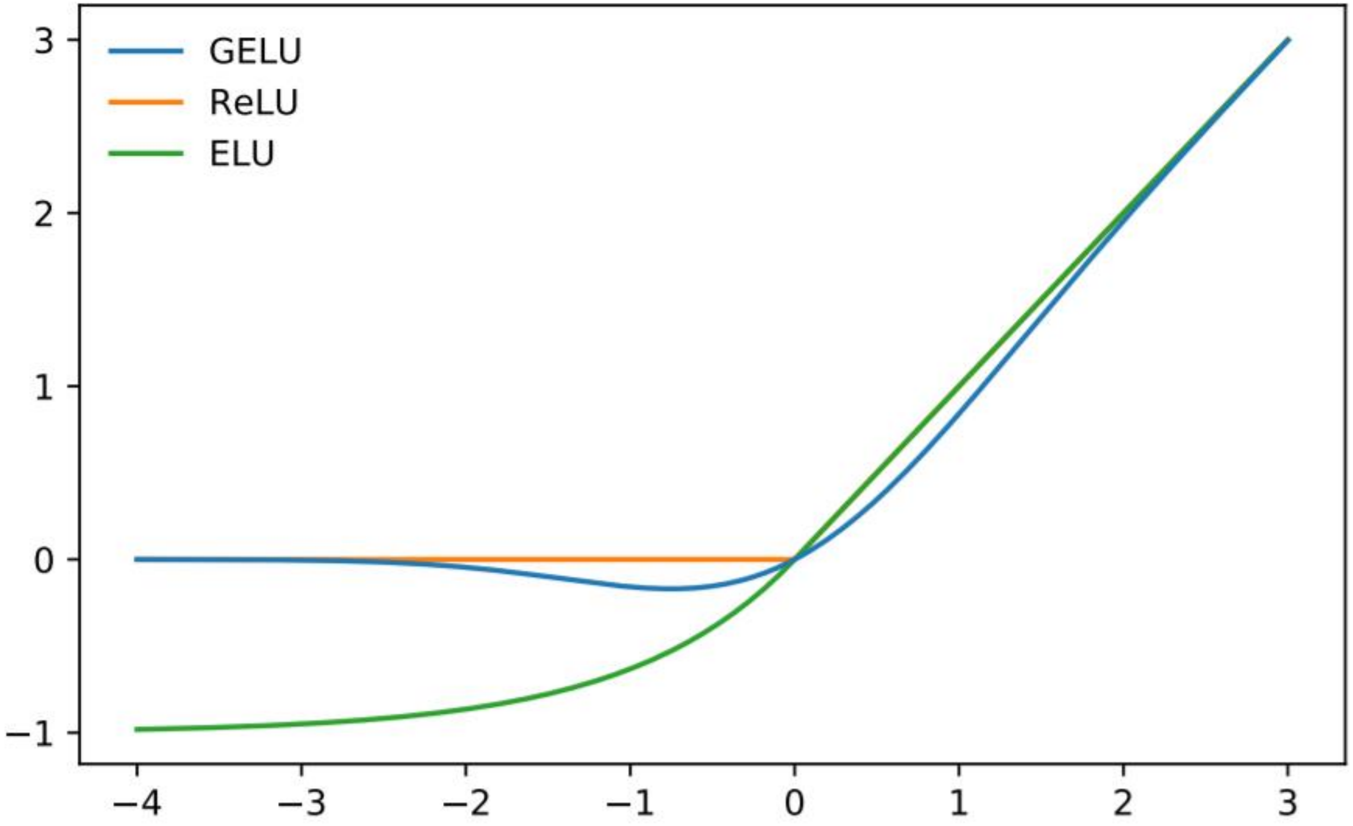

Figure 1: The GELU ($\mu = 0, \sigma = 1$), ReLU, and ELU ($\alpha = 1$).

Experimental Designs

3 datasets to cover various recognition tasks of different granularities

- **Image-level** ImageNet-1K classification (1.28M images; 1000 classes).
- **Region-level** coco object detection (115K images; 80 classes).
- **Pixel-level** ADE20K semantic segmentation (20K images; 150 classes)

	ImageNet		COCO		ADE20k
	top-1	top-5	$\mathrm{AP}^{\mathrm{box}}$	$\mathrm{AP}^{\mathrm{mask}}$	mIoU
w/o shifting	80.2	95.1	47.7	41.5	43.3
shifted windows	**81.3**	**95.6**	**50.5**	**43.7**	**46.1**
no pos.	80.1	94.9	49.2	42.6	43.8
abs. pos.	80.5	95.2	49.0	42.4	43.2
abs.+rel. pos.	81.3	95.6	50.2	43.4	44.0
rel. pos. w/o app.	79.3	94.7	48.2	41.9	44.1
rel. pos.	**81.3**	**95.6**	**50.5**	**43.7**	**46.1**

Table 4. Ablation study on the *shifted windows* approach and different position embedding methods on three benchmarks, using the Swin-T architecture. w/o shifting: all self-attention modules adopt regular window partitioning, without *shifting*; abs. pos.: absolute position embedding term of ViT; rel. pos.: the default settings with an additional relative position bias term (see Eq. (4)); app.: the first scaled dot-product term in Eq. (4).

(a) Regular ImageNet-1K trained models					
method	image size	#param.	FLOPs	throughput (image / s)	ImageNet top-1 acc.
RegNetY-4G [48]	224^2	21M	4.0G	1156.7	80.0
RegNetY-8G [48]	224^2	39M	8.0G	591.6	81.7
RegNetY-16G [48]	224^2	84M	16.0G	334.7	82.9
EffNet-B3 [58]	300^2	12M	1.8G	732.1	81.6
EffNet-B4 [58]	380^2	19M	4.2G	349.4	82.9
EffNet-B5 [58]	456^2	30M	9.9G	169.1	83.6
EffNet-B6 [58]	528^2	43M	19.0G	96.9	84.0
EffNet-B7 [58]	600^2	66M	37.0G	55.1	84.3
ViT-B/16 [20]	384^2	86M	55.4G	85.9	77.9
ViT-L/16 [20]	384^2	307M	190.7G	27.3	76.5
DeiT-S [63]	224^2	22M	4.6G	940.4	79.8
DeiT-B [63]	224^2	86M	17.5G	292.3	81.8
DeiT-B [63]	384^2	86M	55.4G	85.9	83.1
Swin-T	224^2	29M	4.5G	755.2	81.3
Swin-S	224^2	50M	8.7G	436.9	83.0
Swin-B	224^2	88M	15.4G	278.1	83.5
Swin-B	384^2	88M	47.0G	84.7	84.5

Results on COCO object detection and instance segmentation

腾讯课堂

(a) Various frameworks

Method	Backbone	AP^{box}	AP^{box}_{50}	AP^{box}_{75}	#param.	FLOPs	FPS
Cascade Mask R-CNN	R-50	46.3	64.3	50.5	82M	739G	18.0
	Swin-T	**50.5**	**69.3**	**54.9**	86M	745G	15.3
ATSS	R-50	43.5	61.9	47.0	32M	205G	28.3
	Swin-T	**47.2**	**66.5**	**51.3**	36M	215G	22.3
RepPointsV2	R-50	46.5	64.6	50.3	42M	274G	13.6
	Swin-T	**50.0**	**68.5**	**54.2**	45M	283G	12.0
Sparse R-CNN	R-50	44.5	63.4	48.2	106M	166G	21.0
	Swin-T	**47.9**	**67.3**	**52.3**	110M	172G	18.4

(b) Various backbones w. Cascade Mask R-CNN

	AP^{box}	AP^{box}_{50}	AP^{box}_{75}	AP^{mask}	AP^{mask}_{50}	AP^{mask}_{75}	param	FLOPs	FPS
DeiT-S†	48.0	67.2	51.7	41.4	64.2	44.3	80M	889G	10.4
R50	46.3	64.3	50.5	40.1	61.7	43.4	82M	739G	18.0
Swin-T	**50.5**	**69.3**	**54.9**	**43.7**	**66.6**	**47.1**	86M	745G	15.3
X101-32	48.1	66.5	52.4	41.6	63.9	45.2	101M	819G	12.8
Swin-S	**51.8**	**70.4**	**56.3**	**44.7**	**67.9**	**48.5**	107M	838G	12.0
X101-64	48.3	66.4	52.3	41.7	64.0	45.1	140M	972G	10.4
Swin-B	**51.9**	**70.9**	**56.5**	**45.0**	**68.4**	**48.7**	145M	982G	11.6

Results of semantic segmentation on the ADE20K val and test set

腾讯课堂

ADE20K Method	Backbone	val mIoU	test score	#param.	FLOPs	FPS
DANet [23]	ResNet-101	45.2	-	69M	1119G	15.2
DLab.v3+ [11]	ResNet-101	44.1	-	63M	1021G	16.0
ACNet [24]	ResNet-101	45.9	38.5	-		
DNL [71]	ResNet-101	46.0	56.2	69M	1249G	14.8
OCRNet [73]	ResNet-101	45.3	56.0	56M	923G	19.3
UperNet [69]	ResNet-101	44.9	-	86M	1029G	20.1
OCRNet [73]	HRNet-w48	45.7	-	71M	664G	12.5
DLab.v3+ [11]	ResNeSt-101	46.9	55.1	66M	1051G	11.9
DLab.v3+ [11]	ResNeSt-200	48.4	-	88M	1381G	8.1
SETR [81]	T-Large‡	50.3	61.7	308M	-	-
UperNet	DeiT-S†	44.0	-	52M	1099G	16.2
UperNet	Swin-T	46.1	-	60M	945G	18.5
UperNet	Swin-S	49.3	-	81M	1038G	15.2
UperNet	Swin-B‡	51.6	-	121M	1841G	8.7
UperNet	Swin-L‡	**53.5**	**62.8**	234M	3230G	6.2